Materials Research Express

CrossMark

OPEN ACCESS

RECEIVED
8 December 2022

REVISED
18 April 2023

ACCEPTED FOR PUBLICATION
3 May 2023

PUBLISHED
15 May 2023

PAPER

Effect of zirconium and niobium on the microstructure and mechanical properties of high-strength low-alloy cast steels

M Makeshkumar[1], J Anburaj[2], M Sasi Kumar[3] and A Johnson Santhosh[4,*]

[1] Department of Mechanical Engineering, KPR Institute of Engineering and Technology, Coimbatore, Tamil Nadu, India
[2] Department of Metallurgical Engineering, PSG College of Technology, Coimbatore, Tamil Nadu, India
[3] Department of Aeronautical Engineering, KIT-Kalaignarkarunanidhi Institute of Technology, Coimbatore, Tamil Nadu, India
[4] Faculty of Mechanical Engineering, Jimma Institute of Technology, Jimma, Ethiopia
[*] Author to whom any correspondence should be addressed.

E-mail: makeshmech@gmail.com, janburaj@gmail.com, sasikumar.mak@gmail.com and johnson.antony@ju.edu.et

Keywords: HSLA steel, micro-alloying element, SEM, TEM, mechanical properties

Abstract

The aim of this work is to study the effect of zirconium and niobium on the refinement of grain size and mechanical properties of micro-alloyed cast steels in heat treated conditions. Five micro-alloyed cast steels with different compositions, as steel without microalloying elements and micro-alloyed steel with (i) 0.05% Zirconium (Zr), (ii) 0.05% Zirconium (Zr) and 0.05% Niobium (Nb), (iii) 0.10% Zirconium (Zr), and (iv) 0.10% Zirconium (Zr) and 0.10% Niobium (Nb) were investigated. The heat treated samples are normalized at 1000 °C followed by air cooling and were characterized to study the characteristics of carbide precipitates by SEM and TEM and mechanical properties were evaluated by tensile test as per ASTM A370. Among these five cast steels, steel containing 0.10% Zr and 0.10% Nb showed a higher tensile strength of 1184 MPa and yield strength of 740 MPa with reasonable impact energy of 42 J compared to other steels under the same heat treated conditions. Due to the combined addition of Zr and Nb elements in the micro-alloyed steel, a remarkable improvement of mechanical properties particularly strength and impact energy was observed. As evident from microstructure investigation, these improved mechanical properties in the present steel could be attributed due to the effective refinement of ferritic grain size in the normalized condition.

Introduction

Micro-Alloyed Steels (MAS) are considered potent materials for applications in the automobile industry because they have many superior mechanical properties and better formability compared with conventional carbon steels. The addition of the micro amount of alloying elements like titanium, vanadium, zirconium and niobium plays a key role in strengthening of these steel by precipitation hardening and grain boundary strengthening mechanisms [1–5]. The effect on microstructure and mechanical properties on MAS with combinations of V and Nb content has been studied extensively by many researchers [6–9]. The main purpose of adding micro-alloying elements in the steel is to modify the microstructure consisting of a fine fully ferritic grains instead of a ferrite-pearlite matrix [10–13]. The addition of Zr in the Micro Alloyed Cast Steels (MACS) is to modify the morphology of inclusions from elongated to globular shape, thus improving toughness under the impact load [14]. Many researchers studied the influence of niobium, titanium, and vanadium alloys on the mechanical characteristics and microstructure of MACS [15–19]. Some of the research work reported that high strength low alloy (HSLA) steels with niobium have improved strength than titanium and vanadium micro-alloying elements [20]. However, the effect of Zr and Nb combinations on the microstructure and mechanical properties of MACS is reported in limited work. Taking these findings into account, it can be understood that zirconium has a remarkable effect compared to titanium, vanadium, and niobium in micro-alloyed steels to enhance their mechanical properties [21–26]. This article aims at investigating the influence of zirconium as well as combined with niobium on the metallurgical characterization and mechanical properties of low-carbon cast steel under

Table 1. Chemical composition of NMACS and MACS samples.

Samples	Chemical composition (wt%)								
	C	Si	Mn	S	P	Cr	Mo	Zr	Nb
NMACS	0.20	0.37	0.90	0.020	0.020	0.14	0.010	—	—
MACS 1	0.19	0.35	0.84	0.020	0.020	0.13	0.011	0.05	—
MACS 2	0.20	0.38	0.95	0.021	0.022	0.14	0.009	0.05	0.05
MACS 3	0.21	0.37	0.90	0.020	0.020	0.15	0.011	0.10	—
MACS 4	0.22	0.38	0.91	0.022	0.025	0.13	0.010	0.10	0.10

heat treated conditions. The microstructures of these steels were analyzed using an optical microscope, SEM and TEM. The Impact energy, hardness and tensile properties were evaluated by Impact tests, micro hardness tests and tension tests.

Materials and experimental

Five Samples of Non Micro-Alloyed Cast Steel (NMACS) and Micro-Alloyed Cast Steels (MACS) with 0.05–0.10 wt % Nb and Zr were produced by melting in a 50 kg capacity air induction furnace. The identifications and composition of these five cast steels are reported in table 1. During melting, calculated quantities of raw materials were added into the melting furnace in the order of steel scrap and ferroalloys. When liquid metal attained the required temperature of 1600 °C, calculated micro-alloying elements (0.05% and 0.10%) were added to the molten metal in order to get required composition. Before pouring, the molten was deoxidized in the ladle by the addition of 0.15 wt % of Al and Ca-Si deoxidizing agents. Then, the deoxidized liquid metal of NMACS and MACS was poured into Y block CO_2 sand molds as per ASTM A 774 standard. The dimension of the test bar sample is 230 mm length, 75 mm width and 30 mm thickness. After proper cooling and fettling operations, all the test blocks were subjected to stress relieving treatment at 650 °C prior to abrasive wheel cutting. Then the required dimensions of all the test bar samples were subjected to normalizing treatment by heating at 1000 ° C in a muffle furnace, soaking for 1 h per inch at that temperature followed by air cooling.

The heat treated samples of all the investigated steel castings were machined to required dimensions for tensile tests and impact tests as per ASTM A 370 standard. Tensile tests were conducted using the Aimil universal tensile test machine at ambient temperature at a speed of 1 millimeter per minute. Impact tests were conducted using a Charpy impact test machine with range of 0–300 J at 25 ° C. Hardness tests were performed using a Mitutoyo micro-hardness (VHN) tester machine with 10 kg load and 15 s holding time. The metallographic technique and Nital solution 4% were used to produce NMACS and MACS samples. The microstructural investigations were carried out for all the heat treated steels using OM with an image analyzer, SEM and TEM. After etching with Nital solution 2%, the volume fraction of phases as well as grain size in the present steels were determined by image analyzer software (Metal-Plue software). For TEM investigation, heated samples were thinned to 100 μm and physically polished to 50 μm before being electrically thinned in perchloric acid 10% and ethanol 90% solution. The composition of the precipitates was measured by SEM (LN_2-type detector) with Energy Dispersive Spectroscopy (EDS) and TEM.

Results and discussion

Microstructural investigation of NMACS and MACS in the as-cast condition

Figure 1 shows an optical micrograph of as-cast NMACS. This microstructure reveals widmanstatten ferrite i.e. tooth like structure prior to austenitic grain boundaries along with polygonal ferrite and pearlite. The widmanstatten ferrite is formed due to the non-uniform cooling rate caused by sand molds during solidification. Figure 2 shows optical micrographs of MACS samples in the as-cast condition. All four samples of MACS reveal a typical ferrite (around 80% volume) and pearlite (20% volume) in the matrix in the as-cast condition. From the micrographs of the as-cast samples, it is understood that all the cast steels show a heterogeneous microstructure composed of irregular pearlite along with ferrite grains in the as-cast condition. It is also found that the NMACS shows a considerable volume percentage of Widmanstatten ferrite grains along with irregular ferrite in the matrix as compared with the MACS samples. In addition, the volume of pearlite was found to be relatively high in the NMACS sample compared to the MACS samples. It is clear that no polygonal ferrite is observed in the as-cast steel samples due to uneven cooling. This suggests that to refine their microstructure, as-cast steels need to undergo a particular heat treatment process, which improves their mechanical properties and eliminates the presence of micro-segregations in the matrix [27, 28].

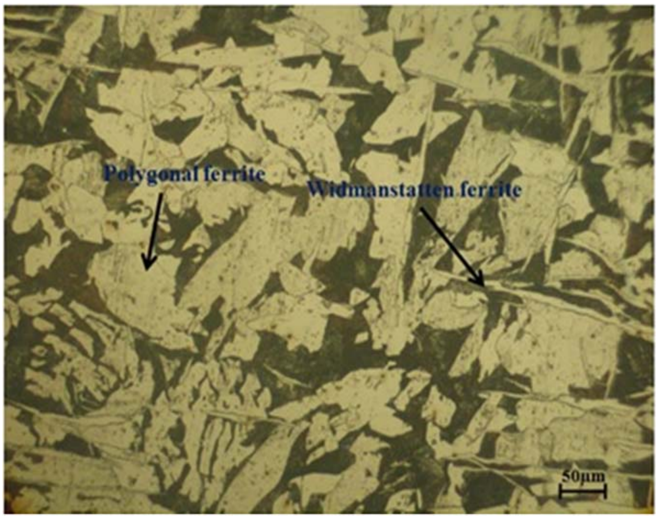

Figure 1. Optical micrograph of NMACS sample in the as-cast condition.

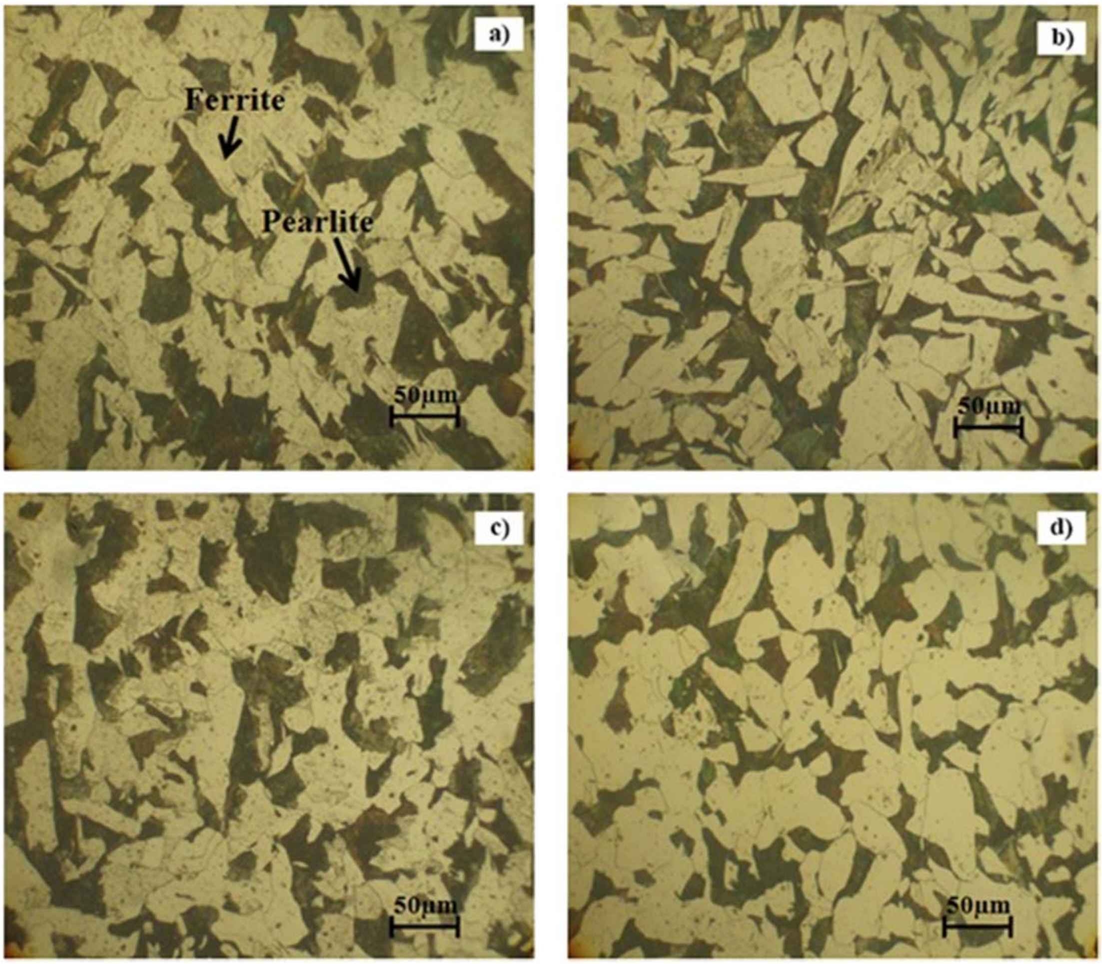

Figure 2. Optical micrographs of MACS samples in the as-cast condition: (a) MACS 1, (b) MACS 2, (c) MACS 3 and (d) MACS 4.

Microstructural investigation of NMACS and MACS in the normalized condition

Optical micrographs of NMACS and MACS in the normalized condition are shown in figure 3. From these micrographs, it is understood that all the normalized cast steels show equiaxed grains consisting of pearlite and ferrite with different volume proportions. From these micrographs, it is observed that the volume percentage of

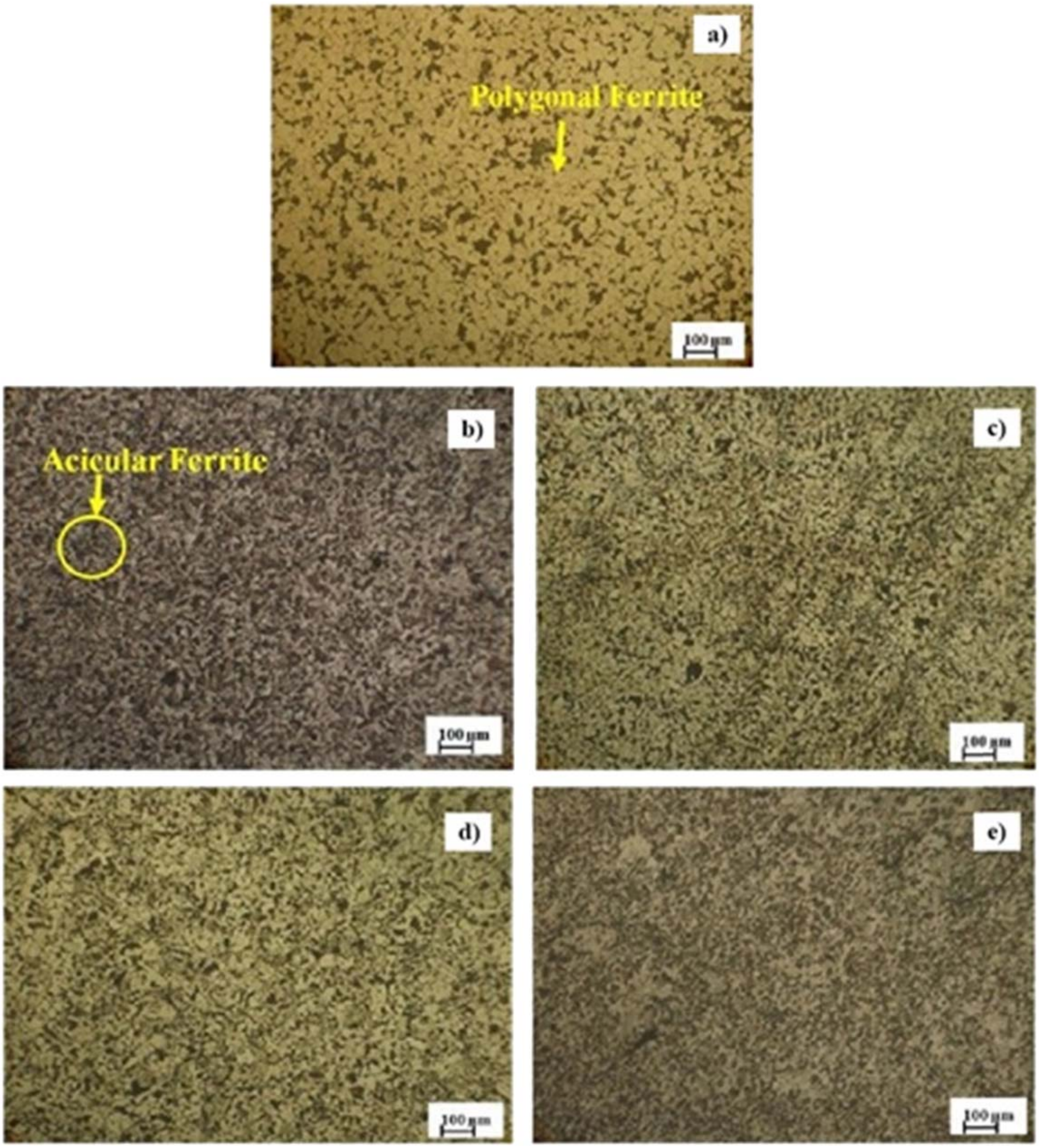

Figure 3. Optical micrographs of NMACS and MACS in the normalized condition (a) NMACS, (b) MACS 1, (c) MACS 2 , (d) MACS 3 and (e) MACS 4.

the ferrite phase in MACS increases with the increasing weight percentage of Zr and Nb elements. This statement is in good concurrence with the result of Wen *et al* [27], who reported that the volume of ferrite in MAS increases with increasing ferrite forming elements. In the case of NMACS, the optical micrograph shows around 85 vol. % of ferrite and the rest pearlite free fromWidmanstatten ferrite (figure 3(a)). However, the volume proportion of phases in MACS differs from that of NMACAS. As evidenced in figure 3(b), it is observed that the optical micrograph of MACS 1 sample reveals fine grained structure consisting of polygonal ferrite (around 85 vol. % of ferrite and the rest of pearlite) However, the optical micrograph of MACS 3 confirms the occurrence of acicular ferrite in the fine grained ferritic matrix (figures 3(b) and (d)). The optical micrograph of MACS 2 and MACS 4 samples shows fine grains of ferrite and pearlite. In addition, the volume of ferrite (90 vol. %) in these two samples of MACS 2 and MACS 4 (figures 3(c) and (e)) is relative higher compared to samples of MACS 1 and MACS 3 (figures 3(b) and (d)). As the amount of zirconium and niobium increases from 0.05 wt % to 0.10 wt %, the volume percentage of ferrite structure in these two samples also increases. The fomartion of zirconium carbo-nitrides precipitation causes ferritic grains to nucleate at a faster rate during heat treatment.

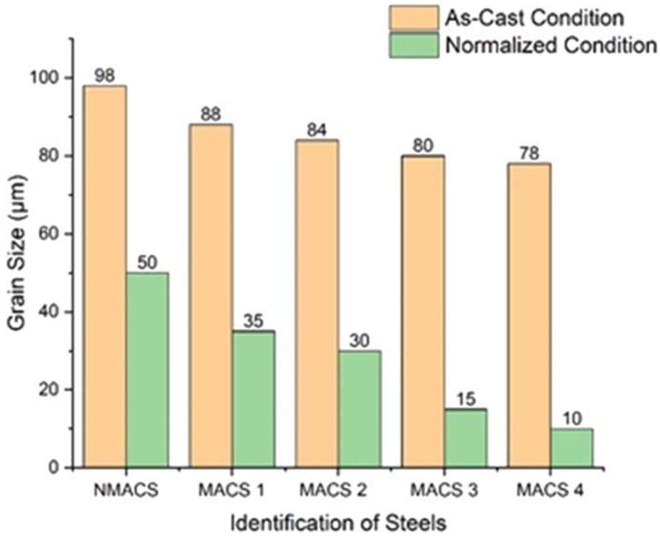

Figure 4. Mean grain size of NMACS and MACS samples.

Table 2. Mean grain size of ferritic grains for NMACS and MACS samples.

Identification of cast steel	Steel with specific alloying elements	Grain size in the as-cast condition (di, μm)	Grain size in the normalized condition (di, μm)
NMACS	Cast steel	98 ± 5	50 ± 5
MACS 1	Cast steel + 0.05% Zr	88 ± 5	35 ± 5
MACS 2	Cast steel + 0.10% Zr	84 ± 5	30 ± 5
MACS 3	Cast steel + 0.05% Zr + 0.05% Nb	80 ± 5	15 ± 5
MACS 4	Cast steel + 0.10% Zr + 0.10% Nb	78± 5	10± 5

Grain size measurement for heat treated steels

Grain size measurement was carried for as-cast as well as heat treated samples using optical microscope with Image analyzer software. The mean grain size are measured for the samples of NMACS, MACS 1, MACS 2, MACS 3 and MACS 4 in the as-cast condition and heat treated condition are shown in table 2 and figure 4. As compared to heat treated samples, the as-cast samples showed coarse grains with irregular shape. The presence of coarse grains with irregular shapes in the as-steel samples could be caused by slow cooling and uneven cooling rates in the sand moulds. From table 2, the grain size of MACS 4 sample is found to be 10 μm level, which is significantly reduced by the addition of micro-alloying elements of Nb and Zr. This could be attributed to the occurrence of zirconium carbide along with niobium carbide in the matrix. As these carbides are thermodynamically more stable at high temperatures, they exert a pinning effect on the grain development of austenite in the normalizing process. These precipitates dissolve by losing the effect of zirconium as a grain refiner. The volume of ferrite in MACS was found to be significantly higher compared to that in NMACS. It can be concluded that the volume of ferrite as well as the refinement of ferritic grains in the MACS can be accelerated by additions of both zirconium and niobium as micro-alloying elements. The presence of carbides and carbo-nitrides in the matrix imparts grain refinement when Zr and Nb content are added to low-carbon cast steel [29, 30]. The volume fraction of phases present in the cast steels was measured using image analyzer software. The results of the image analyzer report on the quantification of pearlite and ferrite for the investigated samples under the as-cast and heat treated conditions are reported in table 3.

SEM with EDS analysis

The shape and size of precipitates present in the MACS were characterized by SEM. Figure 5 shows the presence of precipitates in the ferrite–pearlite matrix of MACS 3. As it is evident from the SEM micrograph, the precipitates appear ta o have a spherical shape with a size of 2 μm. In addition, cubic shape precipitates were also

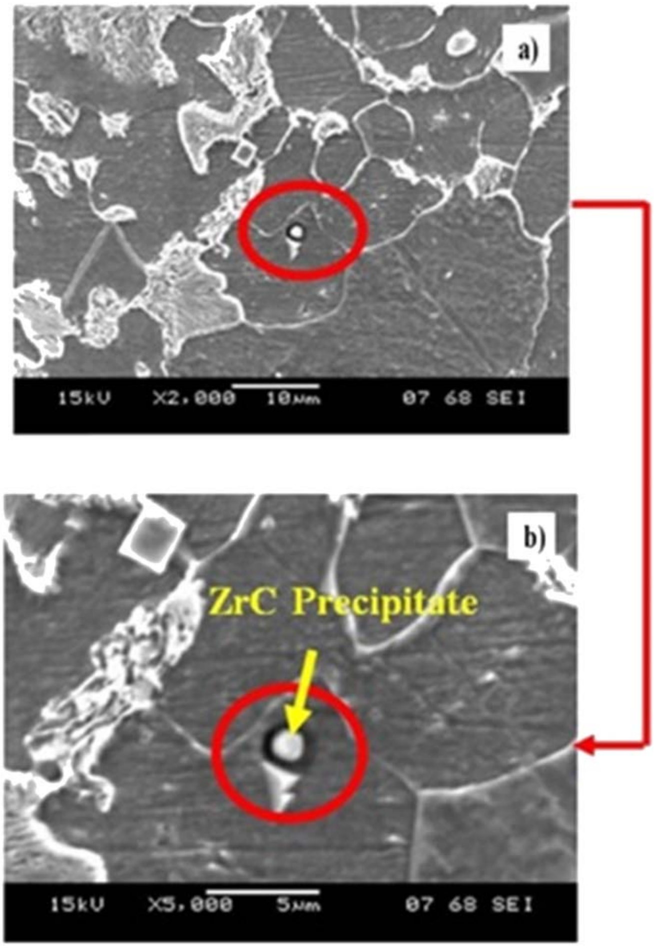

Figure 5. Presence of ZrC precipitates in the ferrite–pearlite matrix of MACS 3.

Table 3. Volume percentage of ferrite and pearlite for NMACS and MACS samples.

Cast steel identification	Volume of phases (%) in the as-cast condition		Volume of phases (%) in the normalized condition	
	Ferrite	Pearlite	Ferrite	Pearlite
NMACS	80 ± 3	20 ± 3	85 ± 3	15 ± 3
MACS 1	85 ± 3	15 ± 3	90 ± 3	10 ± 3
MACS 2	90 ± 3	10 ± 3	94 ± 3	06 ± 3
MACS 3	90 ± 3	10 ± 3	95 ± 3	05 ± 3
MACS 4	90 ± 3	10 ± 3	95 ± 3	05 ± 3

seen in the matrix along with spherical shape precipitates (figure 5(b)). From the SEM micrographs of the MACS samples, it can be understood that the refinement of ferritic grains in the matrix of MACS is owing to the presence of zirconium precipitates and it is in line with the findings of the previous study on similar work [14].

All the heat-treated MACS samples were carried out SEM–EDS analysis to confirm the types of nitrides and carbides precipitates present in the matrix based on their compositions. Figure 6 shows the EDS spectrum of the MACS 3 sample confirming the presence of ZrC precipitates in the ferritic matrix. The chemical composition obtained for ZrC in the MACS 3 sample is matching with the reported value in the literature [6]. Figure 7 shows the SEM micrograph of MACS 4, which exhibits the presence of NbC in the matrix of ferrite and pearlite. The size of the niobium precipitates with cuboid shape noticed in the same sample is around 4 μm which is much smaller than that of the precipitates observed in the other samples. Niobium forms stable carbide and alters the recrystallization temperature of the steel in such a way that the volume of ferrite is significantly increased in the matrix [12].

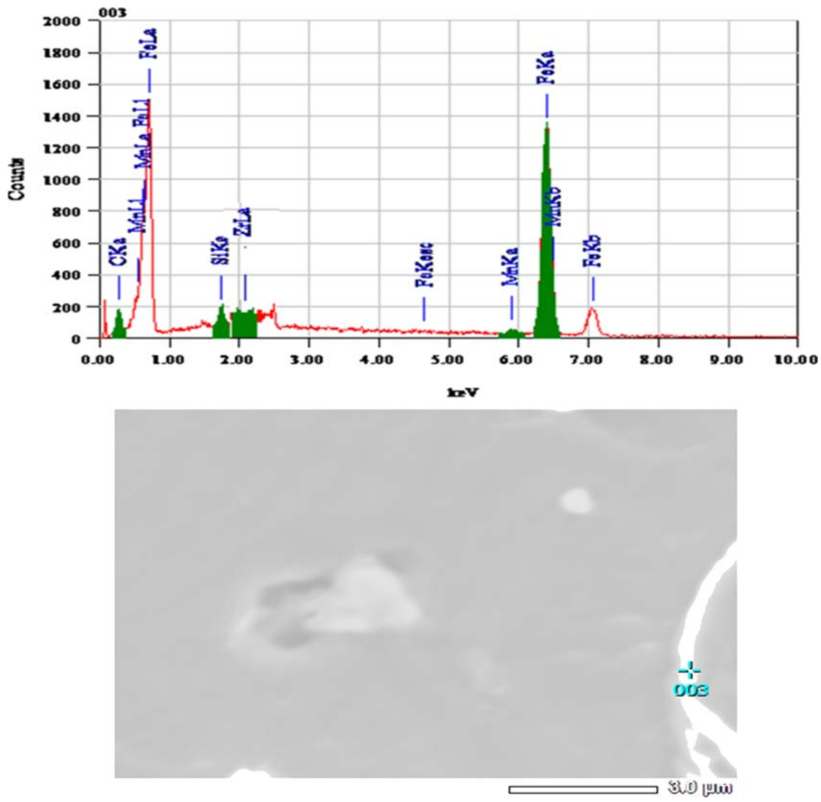

Figure 6. EDS spectrum of the ZrC precipitates along with its SEM micrograph for MACS 3.

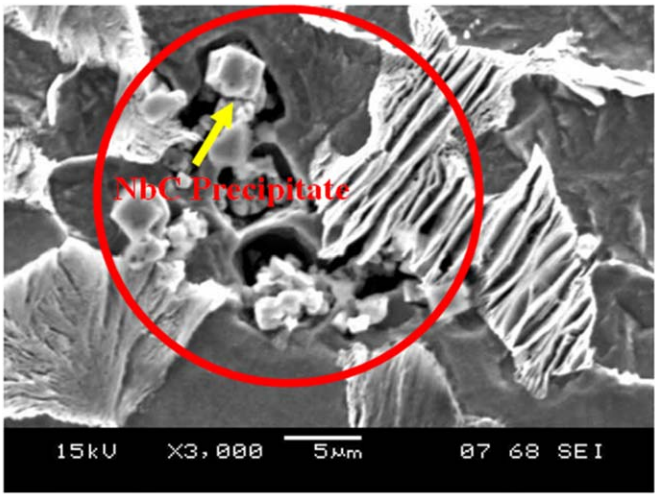

Figure 7. Presence of NbC precipitates in the ferrite–pearlite matrix of MACS 4.

Figure 8 shows the EDS spectrum of NbC precipitates along with their SEM micrograph for MACS 4. As is evident from figure 8, it is confirmed that NbC precipitates are present in the normalized MACS 4. It is also noted that the precipitates are much fine in size and segregated along the prior austenitic grain boundaries. The Nb carbides provide a very good resistance to grain growth during austenitizing and give rise to the formation of fine ferritic grains [14]. This EDS report substantiates the presence of NbC precipitates in the MACS. Figure 9 depicts the TEM micrograph of the MACS 3 sample showing the presence of ZrC precipitates and it is further confirmed with the EDS result.

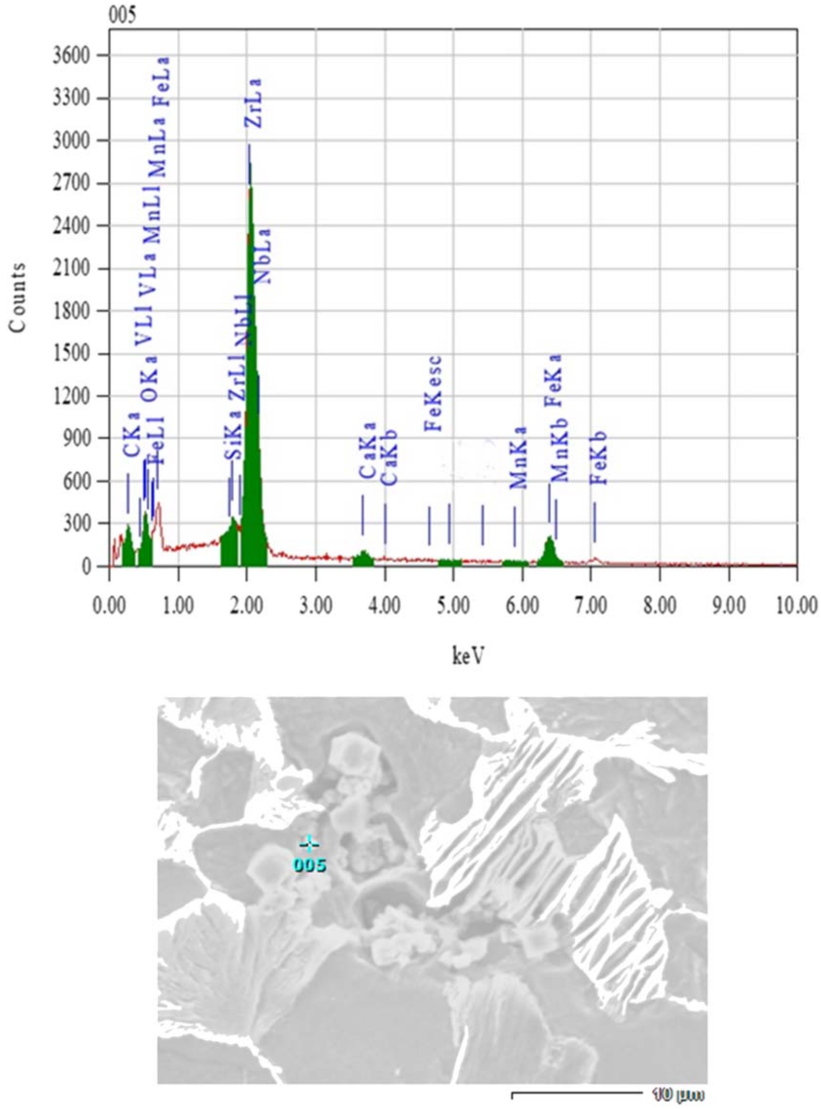

Figure 8. EDS spectrum of the NbC precipitates along with their SEM micrograph for MACS 4.

TEM with EDS analysis

In MACS containing Zr content, two types of precipitates are observed. ZrC precipitates are found at higher temperatures and ZrN precipitates are observed at a lower temperatures [31]. TEM analysis was carried out for the heat-treated samples to ascertain the size, shape and distribution of carbide and nitride precipitates in the matrix of the ferrite-pearlite structure of MACS. Figure 9 shows the fine precipitates of ZrC in the ferritic-pearlite lamellae, which were confirmed by TEM with EDS. It is also noticed that the size of the precipitates is less than 0.5 μm in the MACS 3. For MACS 4, the presence of NbC (<0.5 μm) is observed by TEM as shown in figure 10. The presence of zirconium in the steels reduces the grain size and morphological shifts in carbide precipitates on grain boundaries. This results in a reduction of grain-boundary cracks and slowdown the dislocation along the grain boundaries. The presence of these precipitates is very significant in improving the mechanical properties, in the particular combination of strength and toughness. It is clear evidence that these two samples (MACS 3 and MACS 4) showed very fine grain size (table 2). According to the grain boundary strengthening mechanism, as grain size decreases, strength is increased. This trend is clearly observed in the samples of MACS 3 and MACS 4 (table 5). It is also observed that interlamellar spacing of ferrite and cementite in the pearlite is found to be getting refined in the samples of MACS 3 and MACS 4 (figure 11) due to the presence of these Zr-Nb carbides.

The presence of fine precipitates of NbC in the ferrite lamellae was confirmed by TEM with EDS, which is shown in figure 10. As reported by recent literature work, the addition of niobium in the Zr steels slows down the side plate of ferrite and develops the formation of acicular ferrite [31–33]. Figure 11 shows the TEM micrographs of MACS samples. It is found that the interlamellar spacing of pearlitic structure is refined in steel with the

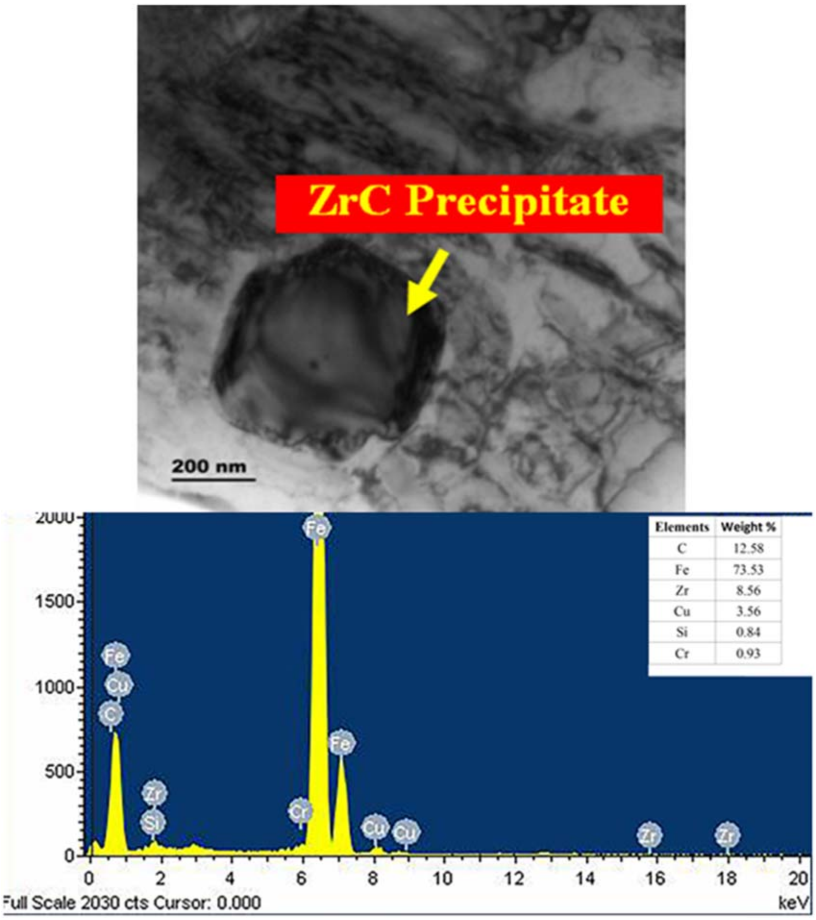

Figure 9. TEM with EDS spectrum of ZrC precipitates in MACS 3.

presence of both Zr and Nb contents. It is clearly evident that the TEM micrographs confirm the refinement of grains in the MACS 4. The addition of micro-alloying elements in low-carbon steel influences a considerable refinement of grains by the formation of fine precipitates either in austenite or austenite to ferrite transformation without altering the constitutions of base microstructures such as ferrite and pearlite in the as-received condition. During normalizing, the carbides or nitrides or carbonitrides can be nucleated at the ferrite-austenite grain boundaries [10].

Mechanical properties evaluation for NMACS and MACS

Mechanical properties including hardness and impact energy as well as tensile properties of the NMACS and MACS samples in the normalized condition are listed in table 4 and 5. Stress-Strain curve for NMACS and MACS samples in the normalized condition are shown in figure 12. Comparing the mechanical properties of NMACS, samples of MACS showed higher yield strength, tensile strength and hardness. This is due to the presence of very fine ferritic grains. As reported in the literature, the precipitation of carbides and carbonitride are responsible for grain refinement which intern gives rise to an increase of strength in MACS. However, the degree of strengthening effect of MACS differs from different types of micro-alloy content and austenitizing temperature [7]. From table 4, it is clearly found that the cast steel with 0.10% Zr and 0.10% Nb (MACS 4) has 1184 MPa ultimate tensile strength with 740 MPa yield strength and 42 J impact energy which is higher than other MACS and NMACS samples.

On the basis of the many previous studies on high strength low alloy steels, Zhang *et al* [8] put forth the relationship of the mechanical properties with the composition and microstructures. The theoretical values of yield strength and tensile strength of the investigated steels were calculated using an empirical equation and it is found that the theoretical values are well supported with the experimental values as reported in table 5. In general, the addition of micro-alloying elements in the low carbon steel influences a considerable refinement of grains by the formation of fine precipitates either in austenite or austenite to ferrite transformation without altering the basic micro constituents such as ferrite and pearlite in the as-received condition. During

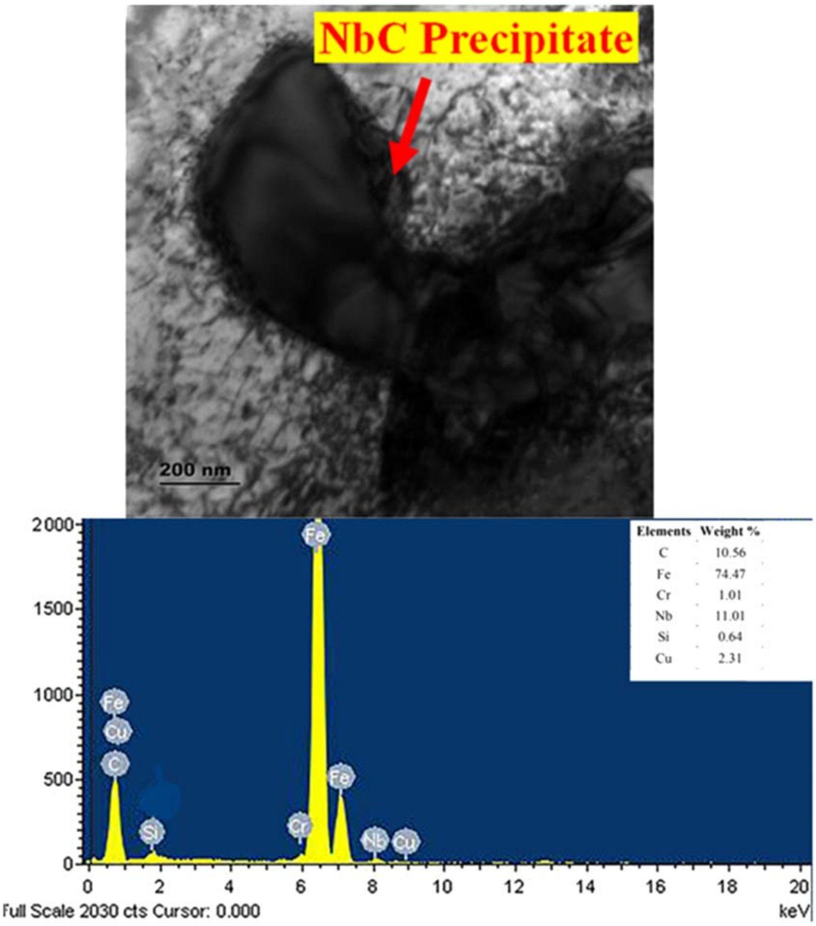

Figure 10. TEM with EDS spectrum of NbC precipitates in MACS 4.

normalizing, the carbides or nitrides or carbonitrides will form at the ferrite-austenite grain boundaries. The uniform distribution of the small size of carbide or carbo-nitride precipitates provides more heterogeneous sites for ferrite formation and refining ferrite grains. However, Zr additions can also increase the transformation temperature of proeutectoid ferrite, delay the pearlitic transformation and then extend the incubation period of ferrite transformation, making the grain size of ferrite become large [7].

$$\text{Yield strength (MPa)} = 15.4\{f\alpha 1/3[2.3 + 3.8(\%\text{Mn}) \\ +1.13\text{d} - 1/2] + (1 - f\alpha 1/3)[11.6 + 0.25\text{So} - 1/2] \\ +4.1[\%\text{Si} + 27.6\sqrt{(\%\text{N})}]\}$$

$$\text{Tensile strength (MPa)} = 15.4\{f\alpha 1/3[16 + 74.2\sqrt{(\%\text{N})} \\ +1.18\text{d} - 1/2] + (1 - f\alpha 1/3) \\ [46.7 + 0.25\text{So} - 1/2] + 6.31\%\text{Si}\}$$

Where

$f\alpha$ - volume fraction of ferrite in %

d -ferritic grain size in μm

So- pearlitic spacing in nm

Kejian *et al* [14] reported that the final grain size of ferrite largely depends upon the size of the precipitates and the transformation temperature of the ferrite. In this study, when Zr content alone exceeds more than 0.05 wt %, the size of ferritic grains becomes coarsened, but it is very fine when the Zr content is combined with Nb. This may be one of the potential reasons, the strength of MACS 3 and MACS 4 is higher without suffering from more toughness than that of MACS 1 and MACS 2.

The tensile strength of MACS samples was increased twice that of the NMACS sample due to the following reasons: (i) high volume of ferrite in the grain boundaries, (ii) presence of fine ferrite grains, (iii) formation of acicular ferrite, and (iv) occurrence of well pearlite colonies. In general, the improvement of strength and impact energy is gained by fine-grained structure [12, 18, 19].

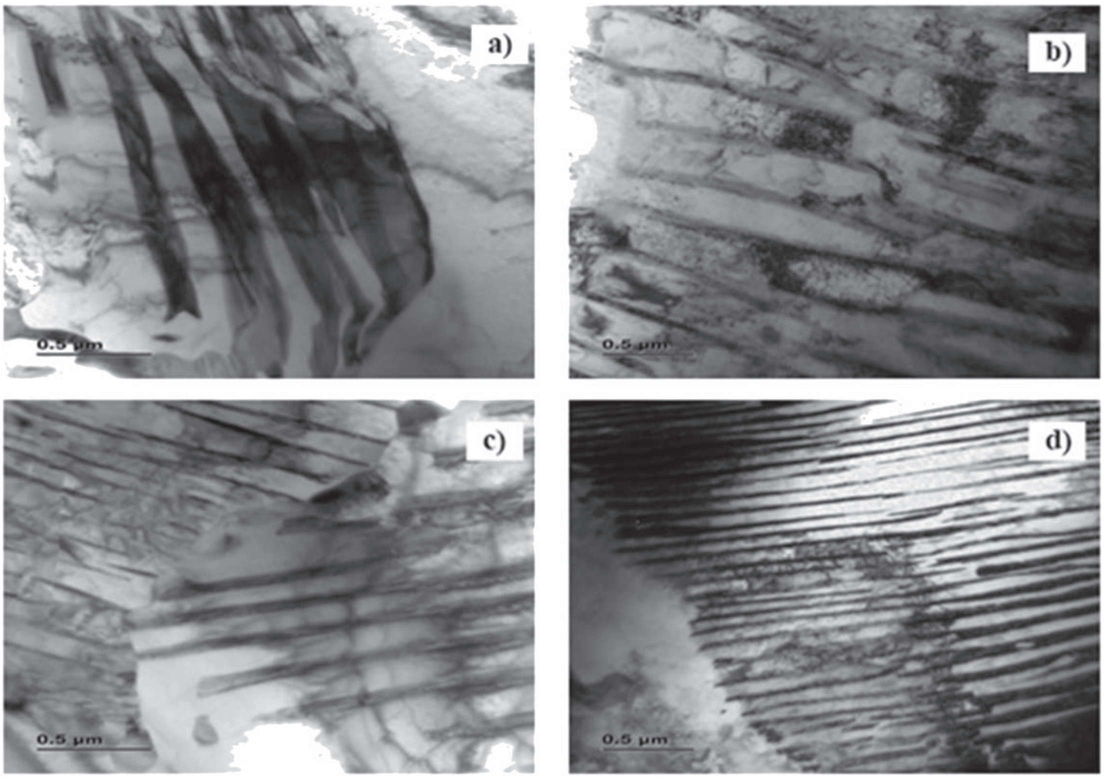

Figure 11. TEM Micrographs of the MACS in the normalized condition: (a) MACS 1, (b) MACS 2, (c) MACS 3 and (d) MACS 4.

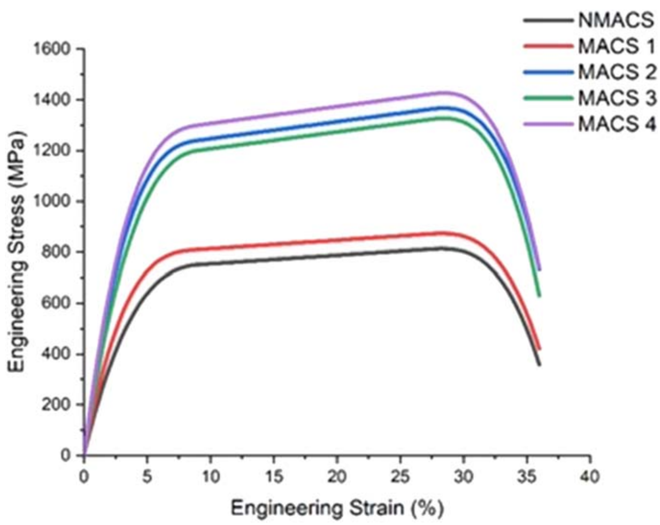

Figure 12. Stress-Strain Curve for NMACS and MACS samples in the normalized condition.

Table 4. Mechanical properties of the NMACS and MACS samples.

	Normalized at 1000 °C				
Mechanical properties	NMACS	MACS 1	MACS 2	MACS 3	MACS 4
Hardness, VHN (load of 10 kg)	184 ± 4	210 ± 4	256 ± 4	232 ± 4	280 ± 4
Impact energy, J	54 ± 5	58 ± 5	45 ± 5	62 ± 5	42 ± 5
Elongation, %	34	32	24	30	22

Table 5. Theoretical and experimental values of the NMACS and MACS samples.

Identification of cast steels	Theoretical Values		Experimental Values	
	Yield Strength (MPa)	Tensile Strength (MPa)	Yield Strength (MPa)	Tensile Strength (MPa)
NMACS	360	624	358	620
MACS 1	422	784	420	780
MACS 2	730	1130	732	1125
MACS 3	635	976	630	980
MACS 4	741	1181	740	1184

Conclusion

Conclusions drawn from microstructural investigations and mechanical properties evaluation are as follows:

- The addition of a small amount (0.1 wt %) of zirconium and niobium in MACS results in the formation of both Zr[C, N] and NbC precipitates. These precipitates retard the growth of ferrite grains during normalizing treatments.
- As evidenced by optical micrographs, it is observed that the presence of Zr content in MACS promotes the formation of acicular ferrite as well as refining the lamellar pearlite in the matrix during normalizing heat treatment.
- SEM and TEM micrographs of MACS samples confirmed the presence of very fine carbides and carbo-nitrides in the matrix of ferrite leading to the refinement of ferritic grains in the normalized condition.
- The mean grain size of MACS 4 is less (10 μm) compared to NMACS, MACS1, MACS2 and MCAS3. This is due to the presence of Zr[C, N] and Nb[C] precipitates.
- The highest tensile strength (1184 MPa) and yield strength (740 MPa) were observed for the sample of MACS 4 compared to other steel samples. This increased strength in MACS 4 is well correlated with microstructure and grain size.

Data availability statement

All data that support the findings of this study are included within the article (and any supplementary files).

ORCID iDs

M Makeshkumar https://orcid.org/0000-0003-0295-1654

References

[1] Sun W and Lu C 2002 Influence of Nb, V and Ti on peak strain of deformed austenite in Mo-based micro-alloyed steels *J. Mater. Process. Tech.* **125-126** 72–6
[2] Ozyurek D, Yıldırım M, Yavuzer B, Simsek I and Tuncay T 2021 The effect of Ni addition on microstructure and mechanical properties of cast A356 alloy modified with Sr *Met. Mater.* **59** 391–9
[3] Rasouli D, KhamenehAsl S, Akbarzadeh A and Daneshi G H 2009 Effects of Ti addition and reheating quenching on grain refinement and mechanical properties in low carbon medium manganese martensitic steel *Mater. Des.* **30** 2167–72
[4] Topcu O and Ubeyli M 2009 On the microstructural and mechanical characterizations of a low carbon and micro-alloyed steel *Mater. Des.* **30** 3274–8
[5] GuangXu X G, Guojun Ma F L and Zou H 2010 The development of Ti-alloyed high strength microalloy steel *Mater. Des.* **31** 2891–6
[6] Chokkalingam B, Raja V, Anburaj J, Immanual R and Dhineshkumar M 2017 Optimization of micro-alloying elements for mechanical properties in normalized cast steel using taguchi technique *Arch. Foundry Eng.* **17** 171–7
[7] Zhao J W and Jiang Z Y 2014 Development of new microalloyed steel by alloying with tungsten *Appl. Mech. Mater.* **716-717** 48–51
[8] Zhang Z H, Liu Y, Zhou Y N, Dong X M, Zhang C X, Cao G H and Gerthsen, D 2018 *Mater. Sci. Eng.*A **738** 203–12
[9] Kalantar M, Najafi H and Afshar R 2019 Effect of precipitation of (Ti, V) N and V (C, N) secondary phases on mechanical properties of V and N microalloyed 1Cr steels *Met. Mater. Int.* **25** 229–37
[10] Hui W, Zhang Y, Shao C, Chen S, Zhao X and Dong H 2015 Microstructural effects on high-cycle fatigue properties of microalloyed medium carbon steel 38MnVS *Mater. Sci. Eng.*A **640** 147–53

[11] Najafi H and Rassizadehghani J 2006 Effects of vanadium and titanium on mechanical properties of low carbon as cast microalloyed steels *Int. J. Cast. Metal. Res.* **19** 323–9
[12] Najafi H, Rassizadehghani J and Halvaaee A 2007 Mechanical properties of as cast microalloyed steels containing V, Nb and Ti *Mater. Sci. Tech.* **23** 699–705
[13] Jana B D, Chakrabarti A K and Ray K K 2003 Study of cast microalloyed steels *Mater. Sci. Tech.* **19** 80–6
[14] He K and Baker T N 1996 Zr-containing precipitates in a TiNbmicroalloyed HSLA steel containing 0.016 wt.%Zr addition *Mater. Sci. Eng.*A **215** 57–66
[15] Pan F, Zhang J, Chen H L, Su Y H, Kuo C L, Su Y H and Hwang W S 2016 Effects of rare Earth metals on steel microstructures *Materials* **9** 1–19
[16] Senberger J, Cech J and Zadera A 2012 Influence of compound deoxidation of steel with Al, Zr, rare Earth metals, and Ti on properties of heavy castings *Arch. Foundry Eng.* **12** 99–104
[17] Wang Q, Sun Y, Zhang C, Wang Q and Zhang F 2018 Effect of Nb on microstructure and yield strength of a high temperature tempered martensitic steel *Mater. Res. Express* **5** 046501
[18] Huo X, Xia J, Li L, Peng Z, Chen S and Peng C-T 2018 A review of research and development on titanium microalloyed high strength steels *Mater. Res. Express* **5** 062002
[19] Shen Y F, Wang C M and Sun X 2011 A micro-alloyed ferritic steel strengthened by nanoscale precipitates *Mater. Sci. Eng.*A **528** 8150–6
[20] Zhao P, Cheng C, Gao G, Hui W, Misra R D K, Bai B and Weng Y 2016 The potential significance of microalloying with niobium in governing very high cycle fatigue behavior of bainite/martensite multiphase steels *Mater. Sci. Eng.*A **650** 438–44
[21] Makeshkumar M and Anburaj J 2019 Study of combined effect of zirconium and titanium on microstructure and mechanical properties of micro-alloyed cast steels *Mater. Res. Express* **6** 1–11
[22] Xie Z J, Ma X P, Shang C J, Wang X M and Subramanian S V 2015 *Mater. Sci. Eng.*A **641** 37–44
[23] Najafi H, Jafar R and Asgar S 2008 Nano-sized precipitation and properties of a low carbon niobium micro-alloyed bainitic steel *Mater. Sci. Eng.*A **486** 1–7
[24] Wang J, Enloe C, Singh J and Horvath C 2016 Effect of prior austenite grain size on impact toughness of press hardened steel *SAE Int. J. Mater. Manf.* **9** 488–93
[25] Bogucki R and Pytel S M 2014 Influence of molybdenum addition on mechanical properties of low carbon HSLA-100 steel *Arch. Metal. Mater.* **59** 859–64
[26] Bloniarz R, Majta J, Trujillo C, Cerreta E and Muszka K 2017 The mechanisms for strengthening under dynamic loading for low carbon and microalloyed steel *Int. J. Impact Eng.* **114** 53–62
[27] Wen X-L, Mei Z, Jiang B, Zhang L-C and Liu Y-Z 2016 Effect of normalizing temperature on microstructure and mechanical properties of a Nb-V microalloyed large forging steel *Mater. Sci. Eng.*A **671** 233–43
[28] Pan T, Chai X-Y, Wang J-G, Su H and Yang C-F 2015 Precipitation behavior of VN microalloyed steels during normalizing *J. Iron. Steel Res. Int.* **22** 1037–42
[29] Zhao J, Lee J H and Yong W 2013 Enhancing mechanical properties of a low-carbon microalloyed cast steel by controlled heat treatment *Mater. Sci. Eng.* **559** 427–35
[30] Dziedzic R D, Muszka K and Majta J 2013 Strain-induced austenitic structure in microalloyed steels *Arch. Metal. Mater.* **58** 745–50
[31] Gao W L, Leng Y, Fu D F and Teng J 2016 Effects of niobium and heat treatment on microstructure and mechanical properties of low carbon cast steels *Mater. Des.* **105** 114–23
[32] Vedani M and Mannucci A 2002 Effects of titanium addition on precipitate and microstructural control in C-Mnmicroalloyed steels *ISIJ Int.* **42** 1520–6
[33] Dou P, Kimura A, Kasada R, Okuda T, Inoue M, Ukai S and Abe F 2014 TEM and HRTEM study of oxide particles in an Al-alloyed high-Cr oxide dispersion strengthened steel with Zr addition *J. Nucl. Mater.* **444** 441–53